

https://doi.org/10.1070/QEL17493

Cross-correlation of phase fluctuations measured with a point source and an incoherent luminous object

N.N. Botygina, O.N. Emaleev, P.A. Konyaev, V.P. Lukin

Abstract. **A high degree of cross-correlation of radiation wavefront aberrations, measured from a point reference source and from an extended object (a system of several luminous points), has been for the first time revealed based on simultaneous measurements of phase fluctuations in optical waves propagating in a turbulent atmosphere. The experimental data are consistent with analytical calculations. The high degree of cross-correlation (above 0.97) of measured phase fluctuations proves that an extended incoherent source can be used as a reference source to ensure the operation of an adaptive focusing system.**

Keywords: *atmosphere, turbulence, correlation wavefront sensor, extended source.*

1. Introduction

Some practical applications are known to be related to the problem of light propagation through an atmosphere; in this case, the atmospheric turbulence and other factors become a serious obstacle for implementing ultimate characteristics and possibilities of optoelectronic systems. Application of adaptive optics (AO) methods makes it possible to significantly reduce these limitations [1–5]. However, the use of AO systems calls generally for an additional source, providing measurements of phase distortions in the radiation propagation channel. This source (referred to as reference) is one of the most important elements of the AO system; it can be designed by different methods. In particular, one can use to this end a natural radiation source; an intentionally formed source; the radiation backscattered from an object; and, finally, the radiation backscattered (or re-emitted) from atmospheric inhomogeneities [5–7]. For example, to solve some problems of astronomy and atmospheric vision systems, a number of studies were devoted to the use of the technique of laser reference stars for image correction [8–10].

Along with the image correction problems, an important problem of optics is to focus coherent light propagating through atmosphere. This objective arises when energy must be delivered to a sufficiently distant object using a laser beam. As different researchers believe, from the point of view of the wave theory of forming light in randomly inhomogeneous media [11], the reference source optimal for focusing coherent light is a point source, i.e., a reference spherical wave [10, 12]. This point source can easily be introduced in theory; however, its practical application may meet some difficulties. In particular, this source has a small size and carries generally a small amount of energy, which hinders the wavefront sensor operation. Another problem related with a point source is the necessity of selecting a useful signal from the environmental background.

N.N. Botygina, O.N. Emaleev, P.A. Konyaev, V.P. Lukin V.E. Zuev Institute of Atmospheric Optics, Siberian Branch, Russian Academy of Sciences, pl. Akad. Zueva 1, 634055 Tomsk, Russia;
e-mail: lukin@iao.ru

Received 27 November 2020
Kvantovaya Elektronika **51** (3) 272–275 (2021)
Translated by Yu.P. Sin'kov

2. Analytical calculations

Even in the end of the 1980s, an idea arose to find some analogue of spherical wave. Previously, the possibility of using a finite-size object as a reference radiation source was analysed in a number of studies [10, 12–18] (by applying the Huygens–Fresnel generalised principle [11]). The reference was considered to be the radiation reflected from the object onto which coherent laser radiation is focused [6, 7, 14–16] or the radiation reflected from atmospheric inhomogeneities [10, 17, 18].

In this context, we analysed the previous experimental studies [19–21] and theoretical calculations [14–16, 22]. In particular, it was shown in those studies that, when performing an analytical analysis, the imaging of an incoherent object under turbulent atmospheric conditions can be replaced with the formation of an incoherent singular radiation beam (based on the application of the generalised Ehrenfest theorem [22]). This incoherent singular beam with an effective radius b, whose coherence function has the form of δ function, can be presented as the sum of several elementary beams propagating from the initial plane. Because of the strong diffraction divergence of the elementary beam, a region of its strong diffraction (but weak turbulent) broadening is formed. Due to the strong diffraction divergence, the size of the elementary beam at the end of atmospheric path becomes much larger than its size at the beginning of the path. As was shown in [16, 22, 23], the dispersion of random displacement of the image of this incoherent beam on an inhomogeneous path in a turbulent atmosphere, σ^2_{image}, measured on a receiving aperture of the effective radius d, is given by the formula

$$\sigma^2_{\text{image}} = 4f^2 \int_0^X \mathrm{d}\xi C_n^2(\xi)\left(1-\frac{\xi}{X}\right)^2 \times\left[\left(1-\frac{\xi}{X}\right)^2 d^2+\left(\frac{\xi}{X}\right)^2 b^2\right]^{-1/6}, \quad (1)$$

where ξ is the current coordinate on the propagation path, $C_n^2(\xi)$ is a function describing the evolution of the refractive index structure parameter along the propagation path, X is

the atmospheric path length, b is the size of incoherent radiation source, d is the detector size (radius), and f is the effective focus of the receiving system.

For a homogeneous atmospheric path, when $C_n^2(\xi)$ is constant, we arrive, with allowance for (1), at the expression:

$$\sigma_{\text{image}}^2 = 4f^2C_n^2X\int_0^1 \mathrm{d}\xi(1-\xi)^2\left[(1-\xi)^2d^2+\xi^2b^2\right]^{-1/6}. \quad (2)$$

An analysis of (2) shows that, for an incoherent beam of small size (with a size b smaller than the detector radius d), the displacements of the beam image and spherical wave coincide; in this case,

$$\sigma_{\text{image}}^2 = \frac{3}{2}f^2C_n^2Xd^{-1/3}, \quad b < d. \quad (3)$$

For an incoherent beam of large sizes ($b > d$), the dispersion of the jitter of incoherent source image ceases to depend on the detector radius and is determined by only the incoherent-source size b:

$$\sigma_{\text{image}}^2 = \frac{27}{8}f^2C_n^2Xb^{-1/3}, \quad b > d. \quad (4)$$

If we consider a vertical atmospheric path with an object located far beyond the atmosphere; introduce an angular size of radiation source, $\Theta_b = b/X$; and let the path length tend to infinity ($X \to \infty$), expression (1) can be written as

$$\sigma_{\text{image}}^2 = 4f^2\int_0^\infty \mathrm{d}\xi C_n^2(\xi)\left[d^2+\xi^2\Theta_b^2\right]^{-1/6}. \quad (5)$$

Formula (5) shows that, in the case of extended inhomogeneous atmospheric paths (e.g., when studying the entire stratum atmosphere), the estimation of the ratio of the detector size d and the angular size of the radiation source, Θ_b, calls for information about the integral optical thickness of atmosphere [11]. This value can be calculated using the function $C_n^2(\xi)$, which describes the evolution of the refractive index structure parameter for a turbulent atmosphere along the propagation path, according to the formula

$$H_{\text{eff}} = \int_0^\infty \mathrm{d}\xi\,\xi C_n^2(\xi)\left(\int_0^\infty \mathrm{d}\xi C_n^2(\xi)\right)^{-1}. \quad (6)$$

For a homogeneous atmospheric path, H_{eff} is equal to the path length.

Thus, theoretical studies [13–16] showed that the image jitter for an extended incoherent object is described practically in the same way as the jitter for a spherical wave (i.e., a point source whose position is determined by the image centroid). The final conclusions about the validity of formulae (1), (2), and (5) were drawn in [22, 23]. Undoubtedly, those conclusions called for experimental confirmation.

At the same time, the number of experiments performed in atmosphere is still limited. The results of experiments carried out on a horizontal atmospheric path and on a vertical path were reported in [19–21] and [22–26], respectively.

3. Experimental setup

Until now, there are barely any data in the literature concerning direct experiments aimed at comparing the results of simultaneous measurements of phase fluctuations for point and extended radiation sources. The main purpose of this work was to carry out such natural experiment.

The main principles of designing a wavefront sensor making it possible to work with an extended object image were reported in [27, 28]. Currently, these sensors (referred to as correlation wavefront sensors), are widely used to study images of extended objects, in particular, when designing AO systems for solar telescopes [29–31]. We have developed a series of these sensors for application in solar telescopes [25, 30]. The high-tech Shack–Hartmann wavefront sensor used in this experiment provided simultaneous measurements of wavefront phase fluctuations for both an extended source and a point reference source.

The extended source was an array of point sources based on laser diodes. This model of incoherent extended source approximately corresponds to the practical case where an object is exposed to solar light and its individual elements have different reflection properties. Under weak illumination conditions, this extended object is observed as an array of luminous points. The optical system is designed so that individual luminous elements of extended incoherent source object are not resolved but each object element can be seen separately.

A schematic of the experimental setup is shown in Fig. 1a. The point coherent source was designed based on an LCS-DTL-317 laser with a wavelength of 0.532 μm and a coherence length above 50 m. The beam diameter at the laser output was 0.27 mm, and the divergence was 2.3 mrad, which provided a beam size of 23 cm at the end of the extended atmospheric path. The incoherent extended light source was formed using several luminous point objects, formed by laser modules KLM-B532-5-5 with a multimode optical fibre 0.4 mm in diameter. The radiation from laser modules was supplied through optical fibres to holes in a metal disk 12 mm in diameter. As a result, the extended incoherent object repre-

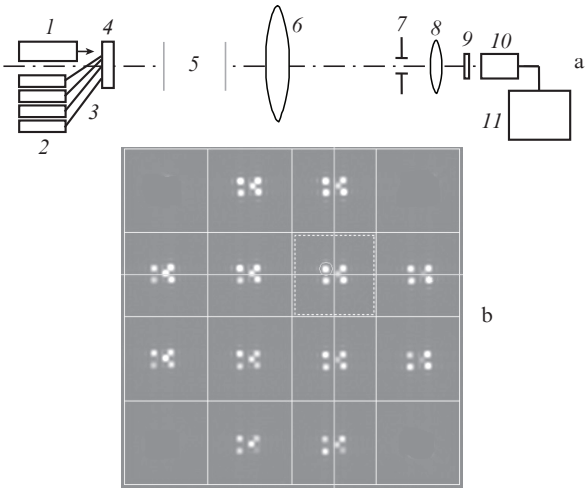

Figure 1. (a) Schematic of the experimental setup and (b) the pattern of focal spots recorded with a Shack–Hartmann sensor:
(*1*) coherent radiation source (laser LCS-DTL-317 with a wavelength of 0.532 μm); (*2*) laser modules KLM-B532-5-5 (radiation wavelength 0.532 μm); (*3*) multi-mode optical fibres (0.4 mm in diameter); (*4*) round disk with holes fixing the positions of all radiation sources; (*5*) atmospheric path; (*6–11*) elements of Shack–Hartmann wavefront sensor [(*6*, *8*) collimator objective and eyepiece, respectively; (*7*) field diaphragm; (*9*) Shack–Hartmann diffraction raster; (*10*) video camera Prosilica; (*11*) computer].

sented a system of several luminous points, which could be reliably reproduced separately (resolved) by the telescope optical system when carrying out observation through a turbulent medium. Measurements were performed for different configurations of holes on the disk surface, i.e., for different systems of luminous points [32]. Different numbers of luminous points (specifically, 2 or 4), arranged differently, were used.

Coherent laser radiation was extracted into atmosphere through the central hole in the disk. The Fresnel parameters of the coherent laser source and the system of luminous object points were, respectively, 0.002 and 0.0102. Control of the output radiation power of laser modules made it possible to choose the necessary brightness of luminous points in order to provide identical conditions for recording images of coherent and incoherent sources. Experiments were performed on a 110-m-long horizontal atmospheric path. Figure 1b shows a photograph of the focal spot pattern (Hartmann pattern) obtained using simultaneously a coherent source (the spot at the centre) and radiation from the laser modules (four focal spots at the periphery).

The phase-fluctuation meter used in our experiments was a Shack–Hartmann wavefront sensor with the following parameters:

diameter of the collimator entrance pupil [position (*6*) in Fig. 1]/mm	98.6
diameter of the collimator exit pupil [position (*8*) in Fig. 1]/mm	3.64
diffraction raster period [position (*9*) in Fig. 1]/μm	814
focal length (mm)	84.7
sensor subaperture size in entrance pupil/μm	22 × 22
number of subapertures in the raster	4 × 4

The Hartmann pattern was recorded using a video camera Prosilica GE680 (640 × 640 pixels, pixel size 7.4 μm). When recording the image displacement, the pixel angular scale reduced to the entrance pupil was 0.67″. Applying quadratic interpolation when determining the position of the correlation function peak, one can measure image displacements accurate to few tenths of a pixel. The diameter of the wavefront sensor entrance aperture is 9.86 cm, and the subaperture diameter is 2.2 cm (the entrance subaperture Fresnel parameter is 6.9).

The video camera frame frequency was 77–87 frames per second, the exposure time of one frame ranged from 130 to 250 μs, the number of recorded frames within one realisation was 5000, and the realisation duration was about 57–65 s.

The data obtained with a wavefront sensor were used to reconstruct phase expansions over Zernike polynomials [33]; this reconstruction was performed synchronously for both a point coherent source and for an extended source formed by several point sources spaced in the transmitter plane. Based on the phase fluctuations, the Fried length for plane and spherical waves was calculated for each experiment. Then the cross-correlation function was calculated for the first mode component with phase-fluctuation expansion numbers of 1–9 [33].

4. Results of measurements in atmosphere

As was said above, the conditions on the atmospheric path were found by measuring the Fried parameter [11]. Different turbulence levels were fixed on the path during measurements. This circumstance allowed us to perform measurements under different conditions. The following values of the Fried parameter r_0 for plane waves were recorded: 32.7, 16.3, and 14.2 mm. This sequence is characteristic of growing turbulence.

In addition, the form of incoherent illuminating object was changed: both an object composed of four luminous sources (forming a square) and a pair of two luminous points were used. The cross-correlation of phase distortions between two incoherent point sources and the correlation between individual sources and their aggregation were investigated in the latter case. Several tens of experiments were performed in total.

The phase distortions of the wavefronts of coherent and extended incoherent sources were measured at the entrance aperture of the optical system (see Fig. 1). The measured phase front was expanded over Zernike polynomials according to [33], and the cross-correlation between the phase-fluctuation polynomials with numbers of 1–9, including the first-order polynomials and third-order polynomials with numbers of 6–9, were calculated. Figure 2 shows the values of the cross-correlation coefficient for the mode components of phase fluctuations, which were measured using both a point reference source and an extended object consisting of four luminous points; the Fried lengths calculated from measurements are also presented. The correlation coefficients for the most important phase components were analysed in the experiment. Synchronous phase measurements of the first Zernike polynomials (these are two slopes, three defocusing components, and four coma components) demonstrate a high degree of cross-correlation for both the extended object and point source. The experimentally found high degree of correlation for the first modes of phase-fluctuation expansion is indeed important, because specifically the first modes carry the main part of the energy of fluctuations, and their high correlation with the fluctuations measured using a point source indicates that measurements of the extended-source image jitter may yield a correct signal with a high correction level.

In particular, it was found that even an object composed of only two spaced incoherent luminous points models fairly correctly the behaviour of an extended incoherent object and can be used to imitate a point reference source.

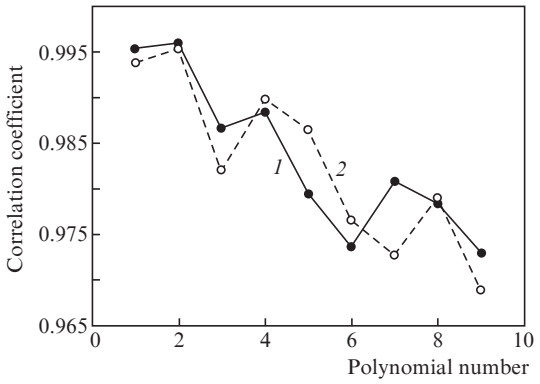

Figure 2. Cross-correlation coefficient for the first nine modes in the expansion of wavefront phase fluctuations over Zernike polynomials for laser radiation and for incoherent object radiation at different turbulence levels; (*1*) the Fried lengths for plane and spherical waves are, respectively, 32.70 and 59.00 mm; (*2*) the Fried lengths for plane and spherical waves are, respectively, 14.20 and 25.60 mm.

The high degree of cross-correlation (above 0.97) obtained in the experiment proves that an object unresolved by a telescope (i.e., considered as a point) and an extended incoherent source can equally efficiently be used as a reference source to provide operation of an adaptive focusing system. The above-described experiments can serve a basis for developing draft proposals for designing a long-range vision correction system. However, the practical implementation of such a system with the aid of a reference source signal should give rise, e.g., to manifestation of backscattering enhancement [34, 35]. In addition, an important factor is the presence of small scatterers (aerosols, solid and liquid precipitates) on an open atmospheric path; due to this, when observing an object through a real aerosol medium [36], only a rather large object can be 'seen' sufficiently clearly to use its image in a correlation wavefront sensor [27, 28]. Therefore, under conditions of strong aerosol scattering, it is rather problematic to provide a high accuracy of phase measurements.

Acknowledgements. The work was carried out with Government funding from the project "Development of methods and systems for adaptive correction for the formation of coherent beams and optical images in the atmosphere" by the Institute of Atmospheric Optics of the Siberian Branch of the Russian Academy of Sciences.

References

1. Babcock H.W. *Publ. Astron. Soc. Pac*., **65**, 229 (1953).
2. Linnik V.P. *Opt. Spektrosk*., (4), 401 (1957).
3. Shapiro J.H. *J. Opt. Soc. Am*., **61**, 492 (1971).
4. Hardy J.W. *Proc. IEEE*, **66** (6), 651 (1978).
5. Kurmaeva A.Kh., Shevchenko V.S. (Eds) *Atmosfernaya nestabil'nost' i adaptivnyi teleskop* (Atmospheric Instability and Adaptive Telescope) (Leningrad: Nauka, 1988).
6. Lukin V.P., Charnotskii M.I. *Materialy VI Vsesoyuznogo simpoziuma po rasprostraneniyu lazernogo izlucheniya v atmosfere* (Proc. VI All-Union Symposium on the Propagation of Laser Radiation in Atmosphere) (Tomsk, 1981) Part 3, p. 83.
7. Lukin V.P., Charnotskii M.I. *Sov. J. Quantum Electron*., **12**, 602 (1982) [*Kvantovaya Elektron*., **9** (5), 952 (1982)].
8. Lukin V.P., Matyukhin V.F. *Sov. J. Quantum Electron*., **13**, 1604 (1983) [*Kvantovaya Elektron*., **10** (12), 2465 (1983)].
9. Foy R., Labeyrie A. *Astron. Astrophys*., **152**, 129 (1985).
10. Lukin V.P., Fortes B.V. *Adaptivnoe formirovanie puchkov i izobrazhenii v atmosfere* (Adaptive Formation of Beams and Images in Atmosphere) (Novosibirsk: Izd-vo SO RAN, 1999).
11. Gurvich A.S., Kon A.I., Mironov V.L., Khmelevtsov S.S. *Lazernoe izluchenie v turbulentnoi atmosfere* (Laser Radiation in a Turbulent Atmosphere) (Moscow: Nauka, 1976).
12. Lukin V.P., Charnotskii M.I. *Opt. Atmos*., **3** (12), 1294 (1990).
13. Kalistratova M.A., Kon A.I. *Izv. Vyssh. Uchebn. Zaved., Ser. Radiofiz*., **9** (6), 1100 (1966).
14. Kon A.I., Mironov V.L., Nosov V.V. *Izv. Vyssh. Uchebn. Zaved., Ser. Radiofiz*., **17** (10), 1501 (1974).
15. Mironov V.L., Nosov V.V. *Izv. Vyssh. Uchebn. Zaved., Ser. Radiofiz*., **20** (10), 1530 (1977).
16. Mironov V.L., Nosov V.V., Chen B.N. *Izv. Vyssh. Uchebn. Zaved., Ser. Radiofiz*., **23** (4), 461 (1980).
17. Ragazzoni R. *Astron. Astrophys*., **305**, L13 (1996).
18. Belen'kii M.S. *Appl. Opt*., **39** (33), 6097 (2000).
19. Kalistratova M.A., Pokasov V.V. *Izv. Vyssh. Uchebn. Zaved., Ser. Radiofiz*., **15** (2), 723 (1972).
20. Gel'fer E.I., Kon A.I., Cheremukhin A.N. *Izv. Vyssh. Uchebn. Zaved., Ser. Radiofiz*., **16** (2), 245 (1973).
21. Banakh V.A., Melamud A.E., Mironov V.L., Nosov V.V., Chen B.N. *Opt. Spektrosk*., **62** (5), 1136 (1987).
22. Nosov V.V. Doct. Diss. (Tomsk, IOA SO RAN, 2009).
23. Nosov V.V. *Proc. X Joint Int. Symp. 'Atm. and Ocean Optics. Atm. Physics'* (Tomsk: IAO SB RAS, 2003) B1.
24. Lukin V.P., Grigor'ev V.M., Antoshkin L.V., Botygina N.N., Emaleev O.N., Konyaev P.A., Kovadlo P.G., Nosov V.V., Skomorovskii V.I. *Opt. Atmos. Okeana*, **22** (5), 499 (2009).
25. Bol'basova L.A, Kovadlo P.G., Lukin V.P., Nosov V.V., Torgaev A.V. *Opt. Atmos. Okeana*, **25** (10), 845 (2012).
26. Lukin V.P. *J. Opt*., **15**, 044009 (2013).
27. Von der Luhe O., Widener A.L., Rimmele Th., Spence G., Dunn R.B., Wiborg P. *Astron. Astrophys*., **224**, 351 (1989).
28. Michau V., Rousset G., Fontanella J.C. *Proc. Workshop on Real-Time and Post-Facto Solar Image Correction* (NSO Sacramento Peak, USA, 1992) pp 91–102.
29. Scharmer G.B. *Proc. SPIE*, **4853**, 4853-52 (2002).
30. Antoshkin L.V., Botygina N.N., Emaleev O.N., Kovadlo P.G., Konyaev P.A., Lukin V.P., Petrov A.I., Yankov A.P. *Opt. Atmos. Okeana*, **15** (11), 1027 (2002).
31. Rimmele T.R. *Living Rev. Solar Phys*., **8**, 92 (2011).
32. Botygina N.N., Emaleev O.N., Lukin V.P. *Proc. SPIE*, **10425**, 10425 OM (2017).
33. Noll R. *J. Opt. Soc. Am*., **66** (3), 596 (1976).
34. Banakh V.A., Gerasimova L.O., Zaloznaya I.V., Falits A.V. *Opt. Atmos. Okeana*, **31** (8), 609 (2018).
35. Banakh V.A., Falits A.V. *Opt. Atmos. Okeana*, **33** (4), 277 (2020).
36. Zuev V.E., Belov V.V., Veretennikov V.V. *Teoriya sistem v optike dispersnykh sred* (Theory of Systems in the Optics of Dispersed Media) (Tomsk: Spektr, 1997).